Understanding Convergence Bids During Blackouts: Analytical Results and Real-World Implications

Ehsan Samani, *Student Member, IEEE* and Hamed Mohsenian-Rad, *Fellow, IEEE*

***Abstract*—Convergence bidding is a financial instrument that is widely adopted in recent years in two-settlement electricity markets to reduce the price gap between the day-ahead market (DAM) and the real-time market (RTM). This paper, for the first time, investigates the operation and impact of convergence bids (CBs) during *blackouts*. First, the amount of load shedding in the RTM is modeled as a *function* of the amount of the cleared CBs in the DAM. The sign of the slope of this function is proposed as a metric to determine if a CB *exacerbates* or *heals* the power outages. Next, a series of mathematical theorems are developed to obtain and characterize this new metric under different network conditions. It is proved that, when there is *no* congestion in the DAM, the metric is always greater than or equal to zero. When there *is* congestion in the DAM, the metric can be positive or negative. Using numerical case studies, we show that, not only when there is no congestion, but also most often when there is congestion, the introduced metric is positive. Therefore, supply CBs almost always hurt the system during blackouts while demand CBs almost always help the system. Furthermore, the impact of load shedding on the profit of CBs is also analyzed. It is shown that, load shedding usually creates advantage for supply CBs and disadvantage for demand CBs in terms of their profit. The implications of these results are discussed. We also analyze the real-world market data from the California Independent System Operator (ISO) during the blackouts in August 2020. It is shown that, the decision by the California ISO to suspend CBs during this event matches the mathematical and numerical results that are obtained and discussed in this paper.**

***Keywords*: Convergence bid, virtual bid, blackout, load shedding, functional model, market data, California ISO.**

NOMENCLATURE

Indices, Sets, and Symbols

N_G	Set of generation bids
i	Index of generation bids
N_L	Set of demand bids
j	Index of demand bids
N_{CB}	Set of convergence bids
j	Index of convergence bids
A, B, C	Subset of generation bids N_G
D, E, F	Subset of demand bids N_L
G, H, I	Subset of convergence bids N_L
$(\cdot)^{min/max}$	Symbol for variables upper/lower limit
$(\cdot)^*$	Symbol for optimal value of a variable

Parameters

$\mathbf{A}, a$	Matrix and diagonal elements of the quadratic coefficients for generation bids in the DAM
$\mathbf{b}, b$	Vector and elements of linear coefficients for generation bids in the DAM
$\mathbf{C}, c$	Matrix and diagonal elements of the quadratic coefficients for demand bids in the DAM
$\mathbf{d}, d$	Vector and elements of linear coefficients for demand bids in the DAM
$\mathbf{M}, m$	Matrix and diagonal elements of the quadratic coefficients for convergence bids in the DAM
$\mathbf{q}, q$	Vector and elements of linear coefficients for convergence bids in the DAM
$\mathbf{v}$	Vector of CBs in the DAM
$\mathbf{E}, e$	Matrix and diagonal elements of the quadratic coefficients for generation bids in the RTM
$\mathbf{k}, k$	Vector and elements of linear coefficients for generation bids in the RTM
$\mathbf{S}$	Matrix of shift factor in the system
$\mathbf{\Psi}$	Incidence matrix for $\mathbf{x}$
$\mathbf{\Theta}$	Incidence matrix for $\mathbf{z}$
$\mathbf{\Omega}$	Incidence matrix for $\mathbf{v}$
$\mathbf{c}$	Vector of transmission line capacities
$\mathbf{L}$	Vector of actual consumption in the RTM

Variables

LS	The total amount of load shedding
CB	The total amount of cleared convergence bids
$\mathbf{s}$	Vector of load shedding at all nodes
$\mathbf{x}$	Vector of generation bids in the DAM
$\mathbf{z}$	Vector of demand bids in the DAM
$\mathbf{v}$	Vector of convergence bids in the DAM
$\mathbf{y}$	Vector of the actual generation in the RTM
δ, λ	Lagrange multipliers of the lower and upper limits of generation and demand in the DAM
ν	Lagrange multipliers corresponding to the power balance equation in the DAM
θ	Lagrange multiplier corresponding to the transmission line constraint in the DAM
π^{DAM}	LMP in the DAM
π^{RTM}	LMP in the RTM

Abbreviations

CB	Convergence Bid
DAM	Day-Ahead Market
RTM	Real-Time Market
LMP	Locational Marginal Price
ISO	Independent System Operator
FCSP	Feasibility Check Subproblem
KKT	Karush-Kuhn-Tucker
APnode	Aggregate Pricing Node
DLAP	Default Load Aggregated Point

The authors are with the Department of Electrical and Computer Engineering, University of California, Riverside, CA, USA, 92521. This work was supported by the National Science Foundation (NSF) grant 1711944. The corresponding author is Hamed Mohsenian-Rad; e-mail: hamed@ece.ucr.edu.

I. Introduction

Convergence bidding, a.k.a., virtual bidding, is a financial market mechanism in two-settlement electricity markets that is used by Independent System Operators (ISOs) to reduce the price gap between the day-ahead market (DAM) and the real-time market (RTM) [1]–[5]. California ISO and all the other ISOs in the United States utilize convergence bids (CBs) [3].

A demand (supply) CB is a bid to buy (sell) energy in the DAM without any obligation to consume (produce) energy. If the CB is cleared in the DAM, then the bidder is charged (credited) at the DAM price and credited (charged) at the RTM price. The *difference* between the earning in the RTM (DAM) and the cost in the DAM (RTM) is paid to the bidder [6].

A. Motivation

While the basic principles of convergence bidding have been studied in the academic literature and industry reports, so far, there has *not* been any study to examine the operation and the impact of convergence bids during major *blackouts*.

Addressing this open problem is critical and necessary. On one hand, as we will show in this paper, there is a drastic change in how CBs affect the electricity markets when there are major power outages. On the other hand, there is a growing trend in the circumstances that cause power outages, such as heat-waves, winter storms, and other climate issues [7].

Therefore, the ISOs are increasingly facing new challenges when it comes to the use of CBs. Accordingly, in this paper, we seek to answer the following research questions: **1)** Despite being a financial tool, does convergence bidding have an impact on the required amount of load shedding during blackouts? **2)** If the answer is 'yes', then how can we understand and explain such impact and its extent and circumstances? **3)** Conversely, is there a relationship between load shedding and the profit of supply CBs and demand CBs during power outages? **4)** Can we use the answers to the above questions to explain why the California ISO decided to entirely suspend CBs for four days during the blackouts which were caused by a major heat-wave in August 2020? **5)** What else can we learn from this real-world incident in California, such as with respect to the profitability and impact of CBs during major power outages?

B. Summary of Contributions and Discoveries

The discoveries and contributions in this paper are as follow:

1) Obtaining rigorous analytical formulations to capture and explain the relationship between load shedding and convergence bidding during power outages. To the best of our knowledge, this is the first paper to study the operation and impact of CBs during power outages.
2) The amount of load shedding in the RTM is modeled as a *function* of the amount of the cleared CBs in the DAM. The sign of the slope of this function is examined as a new metric to determine if a cleared CB is *exacerbating* or *healing* the power outages. We mathematically obtain this metric under different network conditions.
3) It is proved that, when there is *no* congestion in the DAM, the metric is always greater than or equal to zero. When there *is* congestion in the DAM, the metric can be positive or negative. We explain how this can happen based on the parameters of the system. These results clearly show that, despite being financial instruments in the DAM, CBs can affect load shedding in the RTM.
4) We use numerical case studies to confirm the analytical results. Importantly, we show that, not only when there is no congestion, but most often even when there is congestion, the new metric is positive. The conditions for the metric to be negative is very rare. Therefore, we conclude that supply (demand) CBs almost always hurt (help) the system during major power outages.
5) Furthermore, we also examine how load shedding can affect the profit of CBs. Our analysis in this part is again both analytical and numerical. We show that load shedding usually creates advantage for supply CBs and disadvantage for demand CBs in terms of their profit in the electricity market. This might be unfair; because as we previously mentioned, supply CBs exacerbate the power outages while demand CBs heal the outages.
6) The real-world market data from the California ISO during the blackouts in August 2020 are analyzed to better understand the implications of the above results. By analyzing the market data, we show that the decision by the California ISO to suspend CBs during expected outage conditions very well matches the mathematical and numerical results that we obtained in this paper.

C. Literature Review

To the best of our knowledge, there is no other paper that is specifically concerned with understanding the impact of CBs on load shedding or their operation during power outages. However, when it comes to the analysis of CBs under *normal conditions*, i.e., when the network does *not* suffer from major power outages, there *is* a rich body of literature about CBs.

The existing literature can be divided into three groups. First, there are papers that study the impact of CBs on electricity markets under conditions *other than* blackouts [8]–[11]. The impact of CBs on the efficiency of the California ISO market is studied in [8]. In [9], the impact of virtual bids on price volatility in the New York ISO market is examined.

Second, there are papers that are concerned with the potential use of CBs to manipulate the prices in electricity markets, such as in form of market strategies involving financial transmission rights [12], or in form of cyber attacks [13].

Third, there are papers that propose new strategies for convergence bidding to increase the profit for the CB market participant, e.g., see the strategies in [14]–[17].

While there is not much relevance between this manuscript and the papers in the second and the third groups, this paper can be considered to belong to the first group of papers. However, our focus here is on analyzing CBs under the unexplored context of blackouts, which is completely new.

Throughout this paper, we set up our system model based on the core concepts that are adopted in the California ISO market. All our real-world case studies too are based on the California ISO market. Accordingly, there can exist some

relevant features that are used in other markets that we do not consider in this paper. One such example is the concept of scarcity pricing that is used by some ISOs during emergency conditions and blackouts [18]. Scarcity pricing can potentially affect the operation of convergence bids. However, the pros and cons of using sparsity pricing mechanism, as well as whether and how they may have impact on convergence bidding, are beyond the scope of this paper. It should be noted that, there are some recent discussions and debates on whether this particular mechanism does actually work in practice and why it previously did *not* perform as expected, e.g., during the August 2020 blackouts in California [19]–[21].

II. Relationship between Convergence Bidding and Load Shedding

To understand the potential impact of CBs during blackouts, we need to obtain the relationship between the cleared CBs in the DAM and the load shedding in the RTM. This can be done mathematically by expressing load shedding as a *function* of the cleared CBs; as we will discuss throughout this section.

A. Basic Market Formulations

Understanding the role of CBs in electricity markets requires examining both the DAM and the RTM.

First, consider the following DAM optimization problem[1]:

$$\begin{aligned}
\underset{\mathbf{x},\mathbf{z},\mathbf{v}}{\text{minimize}} \quad & (0.5\,\mathbf{x}^T\mathbf{A}\,\mathbf{x}+\mathbf{b}^T\mathbf{x}) - (0.5\,\mathbf{z}^T\mathbf{C}\,\mathbf{z}+\mathbf{d}^T\mathbf{z}) \\
& + (0.5\,\mathbf{v}^T\mathbf{M}\,\mathbf{v}+\mathbf{q}^T\mathbf{v}) && (1)\\
\text{subject to} \quad & \mathbf{1}^T\mathbf{x}-\mathbf{1}^T\mathbf{z}+\mathbf{1}^T\mathbf{v}=0 && (2)\\
& -\mathbf{c} \le \mathbf{S}(\mathbf{\Psi}\,\mathbf{x}-\mathbf{\Theta}\,\mathbf{z}+\mathbf{\Omega}\,\mathbf{v}) \le \mathbf{c} && (3)\\
& \mathbf{x}^{\min} \le \mathbf{x} \le \mathbf{x}^{\max} && (4)\\
& \mathbf{z}^{\min} \le \mathbf{z} \le \mathbf{z}^{\max} && (5)\\
& \mathbf{v}^{\min} \le \mathbf{v} \le \mathbf{v}^{\max} && (6)
\end{aligned}$$

where $\mathbf{x}$ is the vector of generation bids; $\mathbf{z}$ is the vector of demand bids; and $\mathbf{v}$ is the vector of CBs. Matrix $\mathbf{S}$ contains the shift factors in the network; and $\mathbf{c}$ is the vector of transmission line capacities. Matrices $\mathbf{\Psi}$, $\mathbf{\Theta}$, and $\mathbf{\Omega}$ are the incidence matrices for generation bids, demand bids, and CBs, respectively. Matrices $\mathbf{A}$, $\mathbf{C}$, and $\mathbf{M}$ and vectors $\mathbf{b}$, $\mathbf{d}$, and $\mathbf{q}$ are the quadratic and linear coefficients for the generation bids, the demand bids, and convergence bids, respectively.

Once the DAM is cleared, we can obtain the total amount of the cleared CBs in the DAM as follows:

$$CB = \mathbf{1}^T\mathbf{v}^*, \tag{7}$$

where $\mathbf{v}^*$ is the optimal solution in (1)-(5) for the CBs.

[1]Here, we focus on the most fundamental components of the problem formulation in a typical two-settlement electricity market. This helps us gain new insights about the core subject in this paper, with a reasonable and manageable level of details in the mathematical formulations.

Next, consider the following RTM optimization problem:

$$\begin{aligned}
\underset{\mathbf{y}}{\text{minimize}} \quad & 0.5\,\mathbf{y}^T\mathbf{E}\,\mathbf{y}+\mathbf{k}^T\mathbf{y} && (8)\\
\text{subject to} \quad & \mathbf{1}^T\mathbf{y}-\mathbf{1}^T\mathbf{L}=0 && (9)\\
& -\mathbf{c} \le \mathbf{S}(\mathbf{\Psi}\,\mathbf{y}-\mathbf{\Theta}\,\mathbf{L}) \le \mathbf{c} && (10)\\
& \mathbf{x}^{\min} \le \mathbf{y} \le \mathbf{x}^{\max} && (11)\\
& \mathbf{g}(\mathbf{x}^*) \le \mathbf{y} \le \mathbf{h}(\mathbf{x}^*) && (12)
\end{aligned}$$

where $\mathbf{y}$ is the vector of the *actual* generation in the RTM; and $\mathbf{L}$ is the vector of the *actual* consumption in the RTM. Parameters $\mathbf{c}$, $\mathbf{x}^{\min}$, and $\mathbf{x}^{\max}$ are the same as in the DAM problem. Matrix $\mathbf{E}$ and vector $\mathbf{k}$ are the quadratic and linear coefficients of the generation bids in the RTM, respectively.

Regarding notations $\mathbf{g}(\cdot)$ and $\mathbf{h}(\cdot)$ in the constraint in (12), they limit the actual output of the generation units in the RTM based on the outcome of the DAM optimization problem in (1)-(5). Here, $\mathbf{x}^*$ is the optimal generation schedule in the DAM. Functions $\mathbf{g}(\cdot)$ and $\mathbf{h}(\cdot)$ are set for each generator based on its operational requirements [22]. For example, some generators, e.g., nuclear plants, cannot physically lower their actual output below their optimal DAM schedule. As a special case, one can set $\mathbf{g}(\mathbf{x}^*) = \mathbf{x}^*$ and $\mathbf{h}(\mathbf{x}^*) = \mathbf{x}^{\max}$, which in that case, the formulation in (8)-(12) matches the one in [6]. However, our analysis in this paper is general; and we do not need to choose any specific form for functions $\mathbf{h}(\cdot)$ and $\mathbf{g}(\cdot)$. Our only assumption is that, for each generator i, we have $g_i(\cdot) < h_i(\cdot)$, i.e., the lower bound cannot exceed the upper-bound; and function $h_i(\cdot)$ is non-decreasing, i.e., a higher generation schedule in the DAM may not cause a lower upper-bound for the actual generation in the RTM.

B. Analysis of Load Shedding

Once the power grid exceeds its generation capacity or its transmission capacity, load shedding becomes necessary in order to maintain a stable operation. The concept of load shedding is inherently relevant *only* to the real-time operation of the system in the RTM. It is *not* relevant to in the DAM.

In order to analyze the RTM under the circumstances of load shedding, we must examine the *Feasibility Check Subproblem* (FCSP) in the RTM. If the RTM optimization problem in (8)-(12) is infeasible, then it requires load shedding. Of main concern here is the *minimum* amount of load shedding that is required in order to make the RTM optimization feasible:

$$\begin{aligned}
\underset{\mathbf{s},\mathbf{y}}{\text{minimize}} \quad & \mathbf{1}^T\mathbf{s} && (13)\\
\text{subject to} \quad & \mathbf{1}^T\mathbf{y}-\mathbf{1}^T(\mathbf{L}-\mathbf{s})=0 && (14)\\
& -\mathbf{c} \le \mathbf{S}(\mathbf{\Psi}\,\mathbf{y}-\mathbf{\Theta}\,(\mathbf{L}-\mathbf{s})) \le \mathbf{c} && (15)\\
& \mathbf{x}^{\min} \le \mathbf{y} \le \mathbf{x}^{\max} && (16)\\
& \mathbf{g}(\mathbf{x}^*) \le \mathbf{y} \le \mathbf{h}(\mathbf{x}^*) && (17)\\
& \mathbf{s} \ge \mathbf{0} && (18)
\end{aligned}$$

where $\mathbf{s}$ is the vector of minimum required load shedding. The rest of the notations in (13)-(18) are the same as those in the basic RTM optimization problem in (8)-(12).

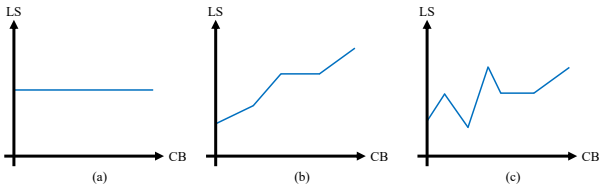

Fig. 1. Three cases for load shedding as a function of cleared CBs: (a) No Impact; (b) Monotone Impact; (c) Non-Monotone Impact.

Once the FCSP is solved, we are interested in examining the total amount of load shedding in the system:

$$LS = \mathbf{1}^T \mathbf{s}^*, \tag{19}$$

where $\mathbf{s}^*$ is the optimal solution of the FCSP in (13)-(18).

C. Impact of Convergence Bids on Load Shedding

Let us define the following *functional* relationship between the amount of the cleared CBs in the DAM and the total amount of load shedding per the FCSP in the RTM:

$$LS = f(CB), \tag{20}$$

where CB is defined in (7) and LS is defined in (19).

Consider the *slope* of the above functional relationship:

$$\frac{\Delta LS}{\Delta CB}. \tag{21}$$

If the *slope* is positive, then an increase in the amount of the cleared CBs results in *more* load shedding in the system. If the *slope* is negative, then an increase in the amount of the cleared CBs results in *less* load shedding in the system.

In this regard, we can distinguish three cases with respect to the impact of cleared CBs on the amount of load shedding:

Case 1 (No Impact): There is no relation between the total amount of load shedding and the amount of the cleared CBs. Accordingly, the *slope* in (21) is always zero, and function $f(\cdot)$ is always *flat*, see Fig. 1(a). Interestingly, this case matches the implicit assumption in the existing literature about CBs. Since CBs are financial instruments in the DAM, while load shedding is a physical action in the RTM, it is generally assumed that CBs do *not* have any impact on load shedding.

Case 2 (Monotone Impact): There is a direct and monotone relationship between the total amount of load shedding and the amount of the cleared CBs. If the relationship is monotone increasing, then the *slope* in (21) is always positive. If the relationship is monotone decreasing, then the *slope* in (21) is always negative. An example for a monotone relationship is shown in Fig. 1(b), where the *slope* is always positive, i.e., increasing CB always results in increasing LS.

Case 3 (Non-Monotone Impact): Although there *does* exist a direct relationship between the total amount of load shedding and the cleared CBs, the relationship is *not* monotone. Therefore, the sign of the *slope* of function $f(\cdot)$ in (20) may *vary* depending on the amount of the cleared CBs. An example for a non-monotone relationship is shown in Fig. 1(c).

While Case 1 is *not* of concern in this paper, as it does *not* indicate any issue with the CBs as far as their impact on load shedding is concerned, Case 2 and Case 3 are both important and insightful and can be investigated in more details. This important analysis is conducted in Sections III-A and III-B.

D. Impact of Load Shedding on CB Profit

When the network experiences load shedding, the basic formulation of the RTM optimization problem in (8)-(12) changes according to the following revised formulation:

$$\underset{\mathbf{y}}{\text{minimize}} \quad 0.5\,\mathbf{y}^T\mathbf{E}\,\mathbf{y} + \mathbf{k}^T\mathbf{y} \tag{22}$$

$$\text{subject to} \quad \mathbf{1}^T\mathbf{y} - \mathbf{1}^T(\mathbf{L} - \mathbf{s}^*) = 0 \tag{23}$$

$$-\mathbf{c} \le \mathbf{S}(\mathbf{\Psi}\,\mathbf{y} - \mathbf{\Theta}\,(\mathbf{L} - \mathbf{s}^*)) \le \mathbf{c} \tag{24}$$

$$\mathbf{x}^{\min} \le \mathbf{y} \le \mathbf{x}^{\max} \tag{25}$$

$$\mathbf{g}(\mathbf{x}^*) \le \mathbf{y} \le \mathbf{h}(\mathbf{x}^*) \tag{26}$$

where $\mathbf{s}^*$ is the optimal solution of the FCSP in (13)-(18). The above optimization problem is the basis to calculate the LMPs in the RTM. The LMPs are calculated based on the dual variables associated with the constraints in (22)-(26), c.f. [6].

Let us denote the vector of LMPs in the RTM by $\boldsymbol{\pi}^{\text{RTM}}$. Similarly, let us denote the vector of LMPs in the DAM by $\boldsymbol{\pi}^{\text{DAM}}$. The latter is calculated based on the dual variables associated with the constraints in the DAM optimization in (1)-(5). We can use the following vector of *price difference* to determine whether a cleared CB is *profitable* at each bus:

$$\boldsymbol{\pi}^{\text{DAM}} - \boldsymbol{\pi}^{\text{RTM}}. \tag{27}$$

If the difference is positive, then the supply CB is profitable. If it is negative, then the demand CB is profitable.

Similar to the functional relationship in Section II-C, we can examine how the price difference in (27) may change when there is a change in CB. Since load shedding only affects the RTM, it has *no impact* on the prices in the DAM. Therefore, we only need to examine the impact of load shedding on the prices in the RTM, i.e., the impact of LS on $\boldsymbol{\pi}^{\text{RTM}}$. We will discuss this subject in details in Section III-C.

In summary, we seek to understand two types of relationships: 1) the impact of CBs on load shedding; 2) the impact of load shedding on the profits associated with the CBs. These two relationships will build the foundation for us to investigate the operation and the impact of CBs during blackouts.

III. Analytical Results

This section contains our core analytical results. First, we propose two theorems to obtain the slope of function $f(\cdot)$, as defined in (21), under two different operating conditions: *with* and *without* transmission line congestion in the DAM. After that, we will also examine the relationship between load shedding and the profit associated with the cleared CBs.

A. Slope of $f(\cdot)$ with No Congestion in the DAM

Suppose there is no congestion in any transmission line in the DAM. Importantly, we do *not* make any assumption regarding transmission line congestion in the RTM.

Theorem 1: If there is no congestion in the network in the DAM, then regardless of the congestion status in the RTM, the

relationship between the amount of the cleared CBs and the required amount of load shedding is always *monotone*. This can be mathematically expressed as:

$$\frac{\Delta LS}{\Delta CB} \geq 0. \tag{28}$$

In such monotone relationship, increasing (decreasing) a supply CB will result in more (less) load shedding. As a result, a supply (demand) CB will exacerbate (heal) the power outage.

Proof of Theorem 1: Since there is no congestion in the DAM, the inequality constraints in (3) are eliminated. We want to calculate the *slope* of function $f(\cdot)$, which is defined in (21). Accordingly, we can use the infinitesimal version of the chain rule for multi-variable functions to obtain:

$$\frac{\Delta LS}{\Delta CB} = \sum_{i \in N_G} \left(\frac{\Delta LS}{\Delta h_i(x_i^*)} \cdot \frac{\Delta h_i(x_i^*)}{\Delta x_i^*} \cdot \frac{\Delta x_i^*}{\Delta CB} \right), \tag{29}$$

where for each generation unit i, notation x_i^* is the corresponding optimal generation schedule in the DAM optimization problem, and $h_i(x_i^*)$ is the corresponding upper-bound in the inequality constraint in (17) in the FCSP.

There are three *fractions* in the formulation in (29). We claim that the following inequalities hold for these fractions:

$$\frac{\Delta LS}{\Delta h_i(x_i^*)} \leq 0, \quad \forall i \in N_G, \tag{30}$$

$$\frac{\Delta h_i(x_i^*)}{\Delta x_i^*} \geq 0, \quad \forall i \in N_G, \tag{31}$$

$$\frac{\Delta x_i^*}{\Delta CB} \leq 0, \quad \forall i \in N_G. \tag{32}$$

From (29), if these three inequalities are true, then we have (28). In other words, if we can show that the three inequalities in (30)-(32) hold, then the proof of Theorem 1 is complete.

First, consider the inequality in (30). The fraction in this inequality captures the sensitivity of the optimal objective value in the FCSP in (13)-(18) with respect to the upper-bound parameter in the inequality constraint in (17). Since FCSP is a *minimization* problem, and also because increasing $h_i(x_i^*)$ results in *relaxing* the constraint in (17), we can conclude that increasing $h_i(x_i^*)$ cannot result in increasing the optimal objective value in FCSP. In other words, if $\Delta h_i(x_i^*) \geq 0$, then $\Delta LS \leq 0$. Thus, the inequality in (30) is indeed true.

Next, consider the inequality in (31). It is the direct result of the fact that, for each generator i, function $h_i(\cdot)$ is non-decreasing; as we discussed at the end of Section II-A. Thus, no further proof is needed regarding the inequality in (31).

Finally, consider the inequality in (32). Verifying this inequality is *not* straightforward. It requires a detailed mathematical discussion. Therefore, for the rest of this proof, we focus on explaining why the inequality in (32) is true.

Given $\mathbf{x}^*$ as the optimal generation schedule in the DAM optimization problem, let us define the following three sets:

$$A = \{i \mid i \in N_G,\ x_i^{\min} \leq x_i^* \leq x_i^{\max}\}, \tag{33}$$

$$B = \{i \mid i \in N_G,\ x_i^* = x_i^{\min}\}, \tag{34}$$

$$C = \{i \mid i \in N_G,\ x_i^* = x_i^{\max}\}. \tag{35}$$

Similarly, given $\mathbf{z}^*$ as the optimal load schedule in the DAM optimization problem, we define the following three sets:

$$D = \{j \mid j \in N_L,\ z_j^{\min} \leq z_j^* \leq z_j^{\max}\}, \tag{36}$$

$$E = \{j \mid j \in N_L,\ z_j^* = z_j^{\min}\}, \tag{37}$$

$$F = \{j \mid j \in N_L,\ z_j^* = z_j^{\max}\}. \tag{38}$$

Similarly, given $\mathbf{v}^*$ as the optimal CB schedule in the DAM optimization problem, we define the following three sets:

$$G = \{k \mid j \in N_{CB},\ v_j^{\min} \leq v_j^* \leq v_j^{\max}\}, \tag{39}$$

$$H = \{k \mid j \in N_{CB},\ v_j^* = v_j^{\min}\}, \tag{40}$$

$$I = \{k \mid j \in N_{CB},\ v_j^* = v_j^{\max}\}. \tag{41}$$

Accordingly, we can rewrite the equality in (2) as follows:

$$\sum_{i \in A} x_i^* + \sum_{i \in B} x_i^{\min} + \sum_{i \in C} x_i^{\max} - \sum_{j \in D} z_j^* - \sum_{j \in E} z_j^{\min} - \sum_{j \in F} z_j^{\max} + CB = 0. \tag{42}$$

Note that, from (7) and (39)-(41), we have:

$$CB = \sum_{k \in G} v_k^* + \sum_{k \in H} v_k^{\min} + \sum_{k \in I} v_k^{\max} = \mathbf{1}^T \mathbf{v}^*. \tag{43}$$

However, since our goal is to obtain the sensitivity in (32) with respect to CB, we keep CB as an explicit term in (42), i.e., we do *not* expand CB in (42) based on its terms in (43).

From (33) and (36), we do *not* know the value of x_i^* for any $i \in A$, and the value of z_j^* for any $j \in D$. To obtain them, we use the Karush-Kuhn-Tucker (KKT) conditions [23]. From the KKT conditions for the DAM optimization problem in (1)-(6), excluding (3) due to absence of congestion, we have:

$$a_i x_i^* + b_i + \lambda_i^* - \delta_i^* + \nu^* = 0, \quad \forall i \in N_G, \tag{44}$$

$$-c_j z_j^* - d_j + \lambda_j^* - \delta_j^* - \nu^* = 0, \quad \forall j \in N_L, \tag{45}$$

where δ_i and λ_i are the Lagrange multipliers corresponding to constraint $x_i^{\min} \leq x_i$ and constraint $x_i \leq x_i^{\max}$, respectively; δ_j and λ_j are the Lagrange multipliers corresponding to constraint $z_j^{\min} \leq z_j$ and constraint $z_j \leq z_j^{\max}$, respectively; and ν is the Lagrange multiplier corresponding to the equality constraint in (2). As for a_i, b_i, c_j, and d_j, they are the corresponding entries in $\mathbf{A}$, $\mathbf{b}$, $\mathbf{C}$, and $\mathbf{d}$, respectively.

It must be noted that, in addition to (44) and (45), one can also write the KKT conditions in terms of taking the derivatives of the Lagrangian function over v_k for all $k \in N_{CB}$. However, we do *not* need any such equation in our analysis; because we already have CB as an explicit term in (42).

From (33) and (36), we have:

$$\delta_i^* = \lambda_i^* = 0, \quad \forall i \in A, \tag{46}$$

$$\delta_j^* = \lambda_j^* = 0, \quad \forall j \in D. \tag{47}$$

By replacing (46) in (44), and also by replacing (47) in (45), and after reordering the terms, we can obtain:

$$x_i^* = -(b_i + \nu^*)/a_i, \quad \forall i \in A, \tag{48}$$

$$z_j^* = -(d_j + \nu^*)/c_j, \quad \forall j \in D. \tag{49}$$

By placing (48) and (49) in (42), we obtain:

$$-\sum_{i\in A}\frac{b_i}{a_i}-\nu^*\sum_{i\in A}\frac{1}{a_i}+\sum_{i\in B}x_i^{\min}+\sum_{i\in C}x_i^{max}+\sum_{j\in D}\frac{d_j}{c_j}+\nu^*\sum_{j\in D}\frac{1}{c_j}-\sum_{j\in E}z_j^{\min}-\sum_{j\in F}z_j^{max}+CB=0. \quad (50)$$

By obtaining ν^* from (50) and then replacing it in (48) for each generator $i\in A$, we can obtain:

$$x_i^*=-\frac{b_i}{a_i}-\frac{1}{a_i}\times\left(1/\left[\sum_{i\in A}\frac{1}{a_i}-\sum_{j\in D}\frac{1}{c_j}\right]\cdot CB+1/\left[\sum_{i\in A}\frac{1}{a_i}-\sum_{j\in D}\frac{1}{c_j}\right]\cdot\left[\sum_{i\in B}x_i^{\min}+\sum_{i\in C}x_i^{max}-\sum_{j\in E}z_j^{\min}-\sum_{j\in F}z_j^{max}-\sum_{i\in A}\frac{b_i}{a_i}+\sum_{j\in D}\frac{d_j}{c_j}\right]\right). \quad (51)$$

Since the DAM optimization problem is a convex optimization problem, parameter $a_i\geq 0$ for all generators $i\in N_G$ and parameter $c_j\leq 0$ for all loads $j\in N_L$. Thus, we have:

$$\sum_{i\in A}\frac{1}{a_i}-\sum_{j\in D}\frac{1}{c_j}>0. \quad (52)$$

Hence, the coefficient of CB in (51) is always negative; and for any $i\in A$, the optimal solution x_i^* is always a decreasing function of CB. This confirms the inequality in (32).

In summary, the inequalities in (30)-(32) hold. Therefore, the inequality in (28) holds; and the proof is complete. ■

From Theorem 1, when there is no congestion in the DAM, and regardless of the congestion status in the RTM, the amount of cleared CBs has a monotone impact on the amount of load shedding. This matches **Case 2** in Section II-C.

This means that, when the RTM problem is *infeasible*, i.e., when there is a need for load shedding in the RTM, the more cleared CBs in the DAM, the more load shedding in the RTM.

Therefore, if CB is positive (supply), then increasing it will result in *more load shedding*; and if CB is negative (demand), then increasing it will result in *less load shedding*.

Under the circumstances in Theorem 1, supply CBs in the DAM exacerbate load shedding in the RTM.

B. Slope of $f(\cdot)$ with Congestion in the DAM

Next, suppose there *is* transmission line congestion in the DAM. The assumption about transmission line congestion is only regarding the DAM. We do *not* make any assumption regarding transmission line congestion in the RTM.

Theorem 2: If there is transmission line congestion in the DAM, the relationship between the amount of a cleared CB and the amount of load shedding *may or may not* be monotone. In other words, it is possible to have either

$$\frac{\Delta LS}{\Delta CB}\geq 0 \quad (53)$$

or

$$\frac{\Delta LS}{\Delta CB}<0. \quad (54)$$

Whether (53) or (54) holds depends on the system parameters. That is, under some choices of the system parameters, the relationship is *not* monotone. And under some other choices of the system parameters, the relationship *is* monotone.

Proof of Theorem 2: For the purpose of this proof, we assume that congestion is exactly on *one* transmission line in the DAM. We denote the transmission line that is congested in the DAM by index k. Furthermore, we assume that exactly *one* CB is cleared in the DAM. We denote the bus where the CB is cleared by index m. The above scenario is all we need in order to derive a case under which the monotone property does *not* hold under some choices of the system parameters, and it *does* hold under some other choices of the system parameters.

Suppose transmission line k is congested such that the *upper-bound* constraint in (3) is binding. Every other inequality constraint in (3) is *not* binding. Accordingly, we can reduce (3) to the following *scalar* upper-bound constraint:

$$\sum_{i\in N_G}(\mathbf{S}\,\mathbf{\Psi})_{ki}\,x_i-\sum_{j\in N_L}(\mathbf{S}\,\mathbf{\Theta})_{kj}\,z_j+(\mathbf{S}\,\mathbf{\Omega})_{km}\,CB\leq c_k, \quad (55)$$

where $(\mathbf{S}\,\mathbf{\Psi})_{ki}$ denotes the entry at row k and column i of the matrix multiplication $\mathbf{S}\,\mathbf{\Psi}$; $(\mathbf{S}\,\mathbf{\Theta})_{kj}$ denotes the entry at row k and column j of the matrix multiplication $\mathbf{S}\,\mathbf{\Theta}$; and $(\mathbf{S}\,\mathbf{\Omega})_{km}$ denotes the entry at row k and column m of the matrix multiplication $\mathbf{S}\,\mathbf{\Omega}$. From (7), and because bus m is the only bus with a cleared CB in the DAM, we have $CB=v_m$.

As in Section III-A, let us define $A,B,C\subseteq N_G$ as in (33)-(35) and $D,E,F\subseteq N_L$ as in (36)-(38). Since the inequality in (55) is binding, it holds as equality at the optimal solution. From this, together with the results in (33)-(38), we have:

$$\sum_{i\in A}(\mathbf{S}\,\mathbf{\Psi})_{ki}\,x_i^*+\sum_{i\in B}(\mathbf{S}\,\mathbf{\Psi})_{ki}\,x_i^{\min}+\sum_{i\in C}(\mathbf{S}\,\mathbf{\Psi})_{ki}\,x_i^{max}-\sum_{j\in D}(\mathbf{S}\,\mathbf{\Theta})_{kj}\,z_j^*-\sum_{j\in E}(\mathbf{S}\,\mathbf{\Theta})_{kj}\,z_j^{\min}-\sum_{j\in F}(\mathbf{S}\,\mathbf{\Theta})_{kj}\,z_j^{max}+(\mathbf{S}\,\mathbf{\Omega})_{km}\,CB-c_k=0. \quad (56)$$

From (33)-(38), the equality in (2) can be written as:

$$\sum_{i\in A}x_i^*+\sum_{i\in B}x_i^{\min}+\sum_{i\in C}x_i^{max}-\sum_{j\in D}z_j^*-\sum_{j\in E}z_j^{\min}-\sum_{j\in F}z_j^{max}+CB=0. \quad (57)$$

Based on (33) and (36), we do not know the value of x_i^* when $i\in A$ and the value of z_j^* when $j\in D$. In order to obtain these unknowns, we can use the following KKT conditions corresponding to the DAM optimization problem in (1)-(5):

$$a_ix_i^*+b_i+\lambda_i^*-\delta_i^*+\nu^*+(\mathbf{S}\,\mathbf{\Psi})_{ki}\,\theta^*=0,\forall i\in N_G, \quad (58)$$

$$-c_jz_j^*-d_j+\lambda_j^*-\delta_j^*-\nu^*-(\mathbf{S}\,\mathbf{\Theta})_{kj}\,\theta^*=0,\forall j\in N_L, \quad (59)$$

where δ_i and λ_i are the Lagrange multipliers corresponding to constraint $x_i^{\min}\leq x_i$ and constraint $x_i\leq x_i^{\max}$, respectively;

δ_j and λ_j are the Lagrange multipliers corresponding to constraint $z_j^{\min} \leq z_j$ and constraint $z_j \leq z_j^{\max}$, respectively; ν is the Lagrange multiplier corresponding to the equality constraint and θ is the Lagrange multiplier corresponding to the upper-bound transmission line constraint in (55).

From (33), (36), (58), and (59), we can obtain:

$$x_i^* = -(b_i + \nu^* + (\mathbf{S}\,\mathbf{\Psi})_{ki}\,\theta^*)/a_i, \quad \forall i \in A, \tag{60}$$

$$z_j^* = -(d_j + \nu^* - (\mathbf{S}\,\mathbf{\Theta})_{kj}\,\theta^*)/c_j, \quad \forall j \in D. \tag{61}$$

Next, for notational simplify, we define:

$$t_1 := -\sum_{i\in A}\frac{b_i}{a_i} + \sum_{j\in D}\frac{d_j}{c_j} + \sum_{i\in B} x_i^{\min} + \sum_{i\in C} x_i^{max} - \sum_{j\in E} z_j^{\min} - \sum_{j\in F} z_j^{max}, \tag{62}$$

$$t_2 := -\sum_{i\in A}\frac{(\mathbf{S}\,\mathbf{\Psi})_{ki} b_i}{a_i} + \sum_{j\in D}\frac{(\mathbf{S}\,\mathbf{\Theta})_{kj} d_j}{c_j} + \sum_{i\in B}(\mathbf{S}\,\mathbf{\Psi})_{ki}\, x_i^{\min} + \sum_{i\in C}(\mathbf{S}\,\mathbf{\Psi})_{ki}\, x_i^{max} - \sum_{j\in E}(\mathbf{S}\,\mathbf{\Theta})_{kj}\, z_j^{\min} - \sum_{j\in F}(\mathbf{S}\,\mathbf{\Theta})_{kj}\, z_j^{max} - c_k. \tag{63}$$

By replacing (60) and (61) in (57), we can obtain:

$$\nu^*\left(\sum_{j\in D}\frac{1}{c_j} - \sum_{i\in A}\frac{1}{a_i}\right) - \theta^*\left(\sum_{i\in A}\frac{(\mathbf{S}\,\mathbf{\Psi})_{ki}}{a_i} + \sum_{j\in D}\frac{(\mathbf{S}\,\mathbf{\Theta})_{kj}}{c_j}\right) + CB + t_1 = 0. \tag{64}$$

By replacing (60) and (61) in (56), we can obtain:

$$\nu^*\left(\sum_{j\in D}\frac{(\mathbf{S}\,\mathbf{\Theta})_{kj}}{c_j} - \sum_{i\in A}\frac{(\mathbf{S}\,\mathbf{\Psi})_{ki}}{a_i}\right) - \theta^*\left(\sum_{i\in A}\frac{((\mathbf{S}\,\mathbf{\Psi})_{ki})^2}{a_i} + \sum_{j\in D}\frac{((\mathbf{S}\,\mathbf{\Theta})_{kj})^2}{c_j}\right) + (\mathbf{S}\,\mathbf{\Omega})_{km}\, CB + t_2 = 0. \tag{65}$$

In (64), let us refer to the coefficient of ν^* as g_1 and the coefficient of θ^* as g_2. Similarly, in (65), let us refer to the coefficient of ν^* as g_3, the coefficient of θ^* as g_4, and the coefficient of CB as g_5. Accordingly, we can express (64) and (65) in the following simplified forms:

$$\nu^* g_1 - \theta^* g_2 + CB + t_1 = 0, \tag{66}$$

$$\nu^* g_3 - \theta^* g_4 + g_5\, CB + t_2 = 0. \tag{67}$$

By solving the system of linear equations in (66) and (67), we can express ν^* and θ^* as a function of CB. After that, we can replace the results in (60) to obtain:

$$\frac{\Delta x_i^*}{\Delta CB} = -\frac{1}{a_i} \times \left(\frac{g_4 - g_2 g_5}{g_2 g_3 - g_1 g_4}\right) - \frac{(\mathbf{S}\,\mathbf{\Psi})_{ki}}{a_i} \times \left(\frac{g_3 - g_1 g_5}{g_2 g_3 - g_1 g_4}\right). \tag{68}$$

The sign of the above equation can change depending on the choice of the parameters in the system. Based on the values of g_1, g_2, g_3, g_4, and g_5, it is possible that the inequality in (32) holds; which in that case, the inequality in (28) will hold. In that case, the relationship between the amount of the cleared CB in the DAM and the amount of load shedding in the RTM *is* monotone. Based on the values of g_1, g_2, g_3, g_4, and g_5, it is possible that the inequality in (32) does *not* hold, to the extent that the inequality in (28) does *not* hold either; which means the relationship between the amount of the cleared CB in the DAM and the amount of load shedding in the RTM is *not* monotone. We will see examples of both scenarios, i.e., both monotone and non-monotone cases, in Section IV. ■

From Theorem 2, when there is congestion in the DAM, it is possible for the relationship between the amount of cleared CBs and the amount of load shedding to be monotone, as in **Case 2** in Section II-C; or non-monotone, as in **Case 3** in Section II-C. It all depends on the values of the parameters.

In practice, when there is congestion in the DAM, in order to specify which CB will exacerbate the power outage and which CB will heal the power outage, the ISO needs to calculate the values of parameters g_1, g_2, g_3, g_4, and g_5 to determine the sign of the expression on the right-hand-side in (68).

Importantly, as we will see in the numerical case studies in Section IV, the relationship between a cleared CB in the DAM and the load shedding in the RTM is *most often* monotone. In other words, even under the circumstances in Theorem 2, the results are *most often* similar to the results in Theorem 1.

C. Relationship between Load Shedding and CB Profit

Recall from Section II-D that, since load shedding only affects the RTM, it does not affect the LMPs in the DAM. From this, together with the formulation of the price difference in (27), in order to examine the impact of load shedding on CB profit, we only need to examine how $\boldsymbol{\pi}^{\text{RTM}}$ changes when LS changes. Accordingly, we can present two theorems.

Theorem 3: If there is no congestion in the network in the RTM, then the relationship between the amount of the load shedding and the profit of the CBs is always monotone.

This can be mathematically expressed for a supply CB as:

$$\frac{\boldsymbol{\pi}^{\text{DAM}} - \boldsymbol{\pi}^{\text{RTM}}}{\Delta LS} \geq 0. \tag{69}$$

In such monotone relationship, increasing (decreasing) the amount of load shedding will result in more (less) profit for supply (demand) CBs; as a result, a supply (demand) CB will be advantaged (disadvantaged) by the power outage.

Proof of Theorem 3: When there is no transmission line congestion in the RTM, the LMP at any bus in the RTM is equal to the dual variable associated with the power balance constraint in (23), c.f. [6]. Let us define such dual variable by π^{RTM}; where $\boldsymbol{\pi}^{\text{RTM}} = \pi^{\text{RTM}}\mathbf{1}$. Accordingly, we are concerned with obtaining the sign of the following fraction:

$$\frac{\Delta \pi^{\text{RTM}}}{\Delta LS}. \tag{70}$$

From (19), we can rewrite (23) as $\mathbf{1}^T\mathbf{y} - \mathbf{1}^T\mathbf{L} = LS$; thus LS is a parameter in the equality constraint in (23). Let Obj^*

denote the optimal objective value of the RTM optimization problem in (22)-(26). From the subject of *perturbation and sensitivity analysis* in convex optimization, we know that [24]:

$$\pi^{\text{RTM}} = -\frac{\Delta Obj^*}{\Delta LS}. \tag{71}$$

Therefore, by applying the infinitesimal version of the definition of derivative, we can express the fraction in (71) as:

$$\frac{\Delta \pi^{\text{RTM}}}{\Delta LS} = -\frac{\Delta \left(\Delta Obj^*/\Delta LS\right)}{\Delta LS} = -\frac{\Delta^2 Obj^*}{\Delta LS^2}, \tag{72}$$

where the last fraction is the infinitesimal version of the definition of the *second derivative*. Since the RTM optimization problem in (22)-(26) is convex, its objective function is convex and has a *non-negative second derivative* [24]. From this, together with the results in (72), we can conclude that:

$$\frac{\Delta \pi^{\text{RTM}}}{\Delta LS} \leq 0. \tag{73}$$

From (73) and (27), and since load shedding does not affect the prices in the DAM, we can conclude that, the CB profit is a monotone function of the amount of load shedding. ■

From Theorem 3, increasing load shedding during power outages results in increasing the profit for supply CBs and decreasing the profit for demand CBs. This monotone relationship is guaranteed if there is *no* transmission line congestion in the RTM. If there *is* transmission line congestion in the RTM, then we can present the following theorem.

Theorem 4: If there is transmission line congestion in the RTM, then the relationship between the amount of the load shedding and the profit of the CBs *may or may not* be monotone. It is possible for a supply CB to have either

$$\frac{\boldsymbol{\pi}^{\text{DAM}} - \boldsymbol{\pi}^{\text{RTM}}}{\Delta LS} \geq 0 \tag{74}$$

or

$$\frac{\boldsymbol{\pi}^{\text{DAM}} - \boldsymbol{\pi}^{\text{RTM}}}{\Delta LS} < 0. \tag{75}$$

Whether (74) or (75) holds depends on the system parameters. That is, under some choices of the system parameters, the relationship is *not* monotone. And under some other choices of the system parameters, the relationship *is* monotone.

The above theorem is the direct result of the concept of negative injection shift factor in the analysis of LMPs; a concept that is extensively studied in the literature [25], [26]. However, similar to the case in Theorem 2, having a non-monotone relationship is rare; as we will see in Section IV-B.

D. Summary of the Mathematical Results

From Theorems 1 and 3, if there is no transmission line congestion in the system, then we can identify the following issue in the operation of CBs during power outages:

The Issue: On one hand, supply CBs exacerbate the power outages by increasing the required amount of load shedding, while demand CBs heal the power outages by decreasing the required amount of load shedding. On the other hand, load shedding creates advantage for supply CBs by increasing their profit, while it creates disadvantage for demand CBs by decreasing their profit. This situation can be unfair; because it rewards the type of CBs that exacerbate power outages and punishes the type of CBs that heal power outages.

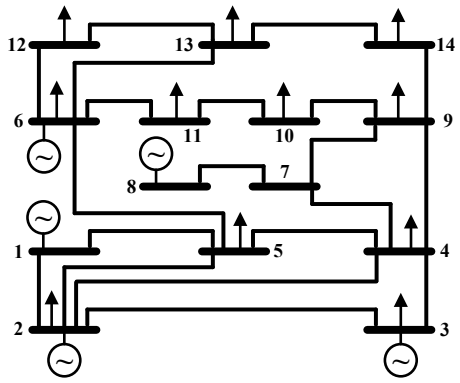

Fig. 2. The IEEE 14-bus standard test system that is studied in Section IV.

From Theorems 2 and 4, if there is congestion in the system, then the above issue may not necessary hold. But, as we will see in Section IV, the relationship between the cleared CBs and the amount of load shedding, as well as the relationship between the amount of load shedding and the profit of CBs are most often monotone. Thus, the above issue most often does hold. In fact, it appears that the above issue was behind a decision by the California ISO to suspend CBs during the outages in August 2020, as we will discuss in Section V.

IV. Numerical Case Studies

In this section, we verify the mathematical results in Section III through numerical case studies. All the numerical case studies are based on the IEEE 14-bus test system, as shown in Fig. 2. The basic characteristics of the generators, loads, and transmission lines are as in [27]. We consider the nominal load at each bus in the IEEE 14-bus test system as the self-scheduling load in the DAM at that bus. In the RTM, we assume 25% increase in the actual load compared to the DAM schedule. The capacity of each transmission line is 45 MW. For the five generators, we have: $\mathbf{A} = \text{diag}(3, 2, 1, 1, 2)$ and $\mathbf{b} = [15, 10, 14, 14, 10]$. The maximum capacity for each generator is 100 MW. We assume that, the generators use the same bids in the RTM as in the DAM, i.e., $\mathbf{E} = \mathbf{A}$ and $\mathbf{k} = \mathbf{b}$.

Regarding functions $\mathbf{g}(\cdot)$ and $\mathbf{h}(\cdot)$ in (12), we assume that: (i) the generator at bus 1 cannot increase its output more than 30% of its DAM schedule, i.e., for this generator, we have: $h(x^*) = 1.3\, x^*$; (ii) the generator at bus 2 cannot increase its output more than 10% of its DAM schedule, and it cannot reduce its generation output to less than its DAM schedule, i.e., for this generator, we have: $h(x^*) = 1.1\, x^*$ and $g(x^*) = x^*$; (iii) for the generator at bus 3, we have: $h(x^*) = 1.2\, x^*$.

A. Relationship between Load Shedding and Cleared CB

In order to *numerically* obtain function $f(\cdot)$ in (20), we change the amount of the CB at a given bus in the DAM within a certain range, and we accordingly solve the DAM optimization problem in (1)-(5), the RTM optimization problem

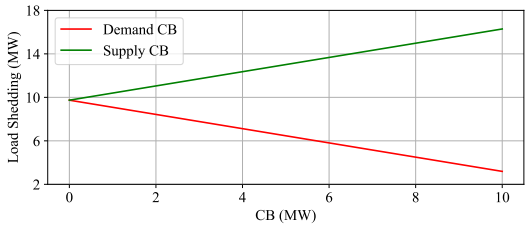

Fig. 3. The numerical results in **Case A**. The results match Theorem 1.

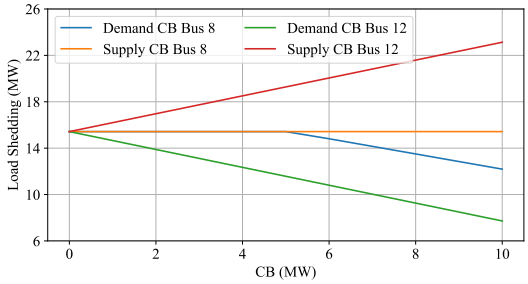

Fig. 4. The numerical results in **Case B**. The results match Theorem 2.

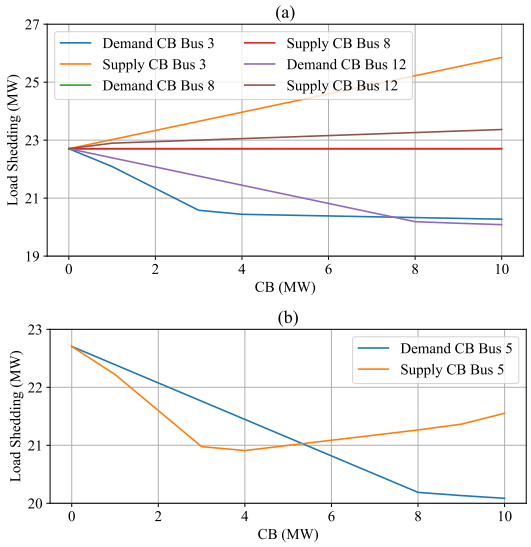

Fig. 5. The numerical results in **Case C**: load shedding as (a) *monotone* function of supply and demand CBs; (b) *non-monotone* function of supply CBs and *monotone* function of demand CBs. The results match Theorem 2.

in (8)-(12), and the FCSP in (13)-(18) to obtain the resulting load shedding in the RTM. We analyze three different cases:

Case A (No Congestion - Monotone Behavior): The results in this case are shown in Fig. 3. Notice that the load shedding is a *monotone increasing* function of the supply CB and a *monotone decreasing* function of the demand CB. To plot these curves, first, we examine a supply CB at an amount that increases from 0 MW to 10 MW. Next, we examine a demand CB from 0 MW to 10 MW. One could interpret the results in Fig. 3 also in terms of changing the CB from -10 MW (demand) to $+10$ MW (supply). The combined curve would be *monotone increasing*. The numerical results in Fig. 3 match the mathematical results in Theorem 1.

Importantly, as we can see in Fig. 3, a supply CB *exacerbates* the power outage by increasing the required amount of load shedding; while a demand CB *heals* the power outage by decreasing the required amount of load shedding.

Case B (Congestion - Monotone Behavior): The results in this case are shown in Fig. 4. The capacity of the transmission lines are 20% *less* than those in Case A. Accordingly, there *is* transmission line congestion in the DAM. At *all* buses, the curves in Fig. 4 are *monotone* functions. The numerical results in Fig. 4 match the mathematical results in Theorem 2. In particular, recall from Theorem 2 that even if some of the transmission lines are congested in the DAM, it is possible that the load shedding in the RTM is a monotone function of the cleared CB at any bus. In this figure, we only see the curves for two buses in the system. The curves for the rest of the buses are not shown; because they simply match one of the curves that are shown in this figure.

For all the buses in Fig. 4, a supply CB *exacerbates* the power outage; while a demand CB *heals* the power outage. Therefore, the ultimate outcome in Case B is similar to Case A, despite having transmission congestion in the DAM.

Case C (Congestion - Non-Monotone Behavior): The results in this case are shown in Fig. 5. The capacity of the transmission lines are 35% less than those in Case A and there *is* transmission line congestion in the DAM.

Fig. 5(a) shows the total load shedding as a function of the cleared CBs at buses 3, 8, and 12. Notice that, all the curves in Fig. 5(a) are monotone. A supply CB at any of these three buses *exacerbates* the power outage while a demand CB *heals* the power outage. Importantly, the monotone behavior that is shown in Fig. 5(a) holds not only at buses 3, 8, and 12, but also at every other bus, *except* at bus 5; as we will see next.

Fig. 5(b) shows the total load shedding as a function of the cleared CB at bus 5. We can see that the load shedding is still being impacted by changing the cleared CB, but it is *not* a monotone function of the cleared supply CB at bus 5.

Next, we discuss the non-monotone behavior in Fig. 5(b). In this case, the added CB causes congestion in the DAM on the transmission line between bus 4 and bus 5. Due to this new congestion, the generation schedule for the generator at bus 3 in the DAM increases (instead of decreasing). Since the output of this unit in the RTM depends on its DAM schedule, this generator will have more output in the RTM when a supply CB is placed at bus 5, which reduces load shedding. This causes the non-monotone behavior in Fig. 5(b), for the range of supply CB between 0 to 4 MW. Ultimately, by increasing the supply CB beyond 4 MW, the output of the generator at bus 3 reaches its maximum capacity in the RTM. As a result, its generation output in the RTM is *no longer* dependent on its DAM schedule. Accordingly, a supply CB at bus 5 that is larger than 4 MW causes the same typical monotone effect on the amount of load shedding that we saw in Cases A and B.

The numerical results in Fig. 5 match the mathematical results in Theorem 2. It is worth emphasizing that, the above non-monotone behavior is *very rare* and it happens only under some very specific circumstances, as we discussed in Theorem 2. In most cases, the monotone behavior *does* hold; but there

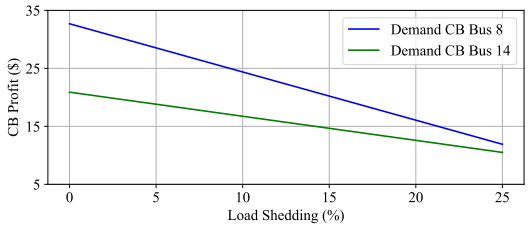

Fig. 6. Impact of load shedding on the profit of CBs at buses 8 and 14.

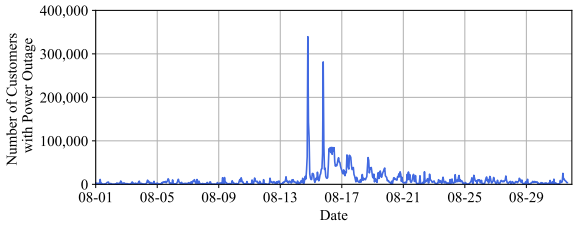

Fig. 7. Hourly number of costumers who lost power during the month of August in the California ISO. The spikes occur on August 14 and 15.

do exist cases for which the monotone behavior does not hold.

B. Relationship between Load Shedding and CB Profit

In Theorem 3 in Section III-C, we mathematically proved that if there is *no* transmission line congestion in the RTM, then load shedding *always* results in decreasing (increasing) the profit of demand (supply) CBs. Therefore, we do not provide any numerical result for the case in Theorem 3. Instead, in this section, we numerically obtain the relationship between load shedding and the profit of CBs in the presence of congestion in the RTM. We use the same setting that we introduced in the beginning of Section IV. The results are shown in Fig. 6. Here, we gradually shed the load at bus 3, to examine the CB profit for placing 1 MWh demand CBs at two different buses. But 3 is selected for load shedding; because it has the largest load in the system. The profit of a supply CB would be exactly the opposite in each case.

As we can see, in both cases, the relationship between the amount of load shedding and the profit of the CB is monotone. Increasing the amount of load shedding results in decreasing the profit of the demand CB. It should be emphasized, that the same results are achieved at any other bus in the system. This is despite the fact that there is congestion in the system.

V. Real-World Case Study

In this section, we discuss a real-world case study related to the power outages that happened in California due to a major heat wave during August 2020. The real-world market data is analyzed to understand different aspects related to the operation and impact of CBs during this case study.

A. Overview of the Case

During August 14 through August 19, 2020, the state of California experienced an extreme heat wave, which significantly increased the load for its residents. The increased stress on the electric power system resulted in a series of rotating blackouts that caused power outages for over 350,000 costumers [28]. Fig. 7 shows the hourly number of costumers who lost power during the month of August [29]. In this figure, the two spikes show the outages that happened during the peak hours:

- 6:00 PM - 9:00 PM on August 14;
- 6:00 PM - 8:00 PM on August 15.

After that, the amount of load shedding gradually decreased, although the number of customers who experienced a power outage remained higher than usual for the next several days.

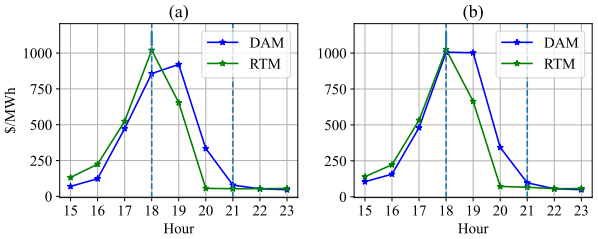

Fig. 8. Comparing the hourly DAM LMPs and the hourly average RTM LMPs on August 14 in two of the three DLAPs in California: a) PG&E; b) SDG&E. The graph for the third DLAP, i.e., SCE, is similar (not shown here).

In this case study, we focus on the analysis of CBs in the aggregated pricing nodes (APnodes) in the California ISO market. In August 2020 and *before* the event, i.e., from August 1 through August 13, a total of 427 APnodes hosted at least one CB at any time during this period. A total of 66 market participants submitted at least one CB to the California ISO market during this period. The total number of submitted CBs was 119,332; out of which 56% were cleared in the market. The total profit that was earned by all the CB market participants during this period was $982,181.

Of interest among the APnodes in California are the three Default Load Aggregation Points (DLAPs): Pacific Gas and Electric (PG&E), Southern California Edison (SCE), and San Diego Gas and Electric (SDG&E). These three major APnodes cover Northern, Central and Southern part of California.

B. Convergence Bids: Analysis of the Prices and the Profits

Fig. 8 shows the hourly LMPs during August 14 in the DLAPs in the California ISO market. The vertical lines in each figure show the start time and the end time of the period of power outage (i.e., severe load shedding). At both DLAPs, we can clearly distinguish two different periods. At the beginning, and up until the start of the outage period, the RTM LMP is *higher* than the DAM LMP; because the network is experiencing a higher load in real-time than expected. However, right around the time that the California ISO started dispatching severe load shedding, the RTM LMPs *suddenly started to drop* and became *lower* than the DAM LMPs.

The exact same situation also happened on August 15, 2020, as soon as the ISO started dispatching the load shedding across the system. The figures are not shown here.

From the above observations, while the demand CBs made profit before the outages, they started losing money as soon as the outages started. This exactly matches our analysis in

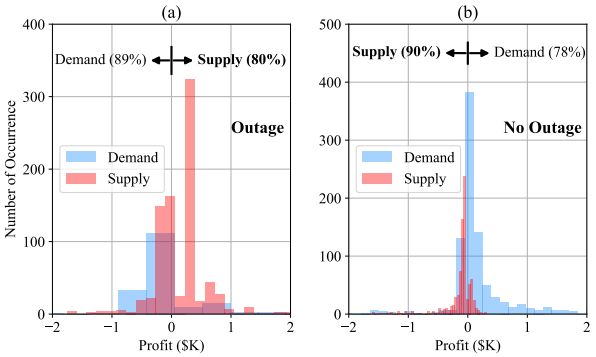

Fig. 9. Comparing the distribution of the CB profits on August 14 and August 15 during (a) the outage hours; (b) same duration but before the outage hours.

Section III-C. Furthermore, this matches the concern that we raised in Section III-D; because the demand CBs, which are the type of CBs that help healing the power outages, are being negatively affected by the power outages.

Next, we examine and compare the profit that is gained by each cleared CB during two different market conditions:

- **During Peak Outage Hours:** From 6:00 PM to 9:00 PM on August 14 and also from 6:00 PM to 8:00 PM on August 15. The results are shown in Fig. 9(a).
- **Right Before Peak Outage Hours:** From 3:00 PM to 6:00 PM on August 14 and also from 4:00 PM to 6:00 PM on August 15. The results are shown in Fig. 9(b).

Notice that, the results in Fig. 9(a) and those in Fig. 9(b) are the *opposite of each other*. In Fig. 9(a), 80% of the supply CBs have *positive* profit; while in Fig. 9(b), 90% of the supply CBs have *negative* profit. Furthermore, in Fig. 9(a), 89% of the demand CBs have *negative* profit; while in Fig. 9(b), 78% of the demand CBs have *positive* profit.

The above results are very insightful and they confirm some of the issues that we raised in Section III-D. To see this, recall from Sections III-A and III-B that in most cases, a supply CB exacerbates the outage circumstances while a demand CB heals the outage circumstances. Accordingly, one would expect that a supply CB is punished during the outages while a demand CB is rewarded during the outages. However, the occurrence of the outages creates a situation that the supply CBs are rewarded while the demand CBs are punished.

It is worth noting that, the California power system was under stress even before the outage period in Fig. 9(b); because the heat wave had already started. However, it had not gone to the level to cause power outages; as in the case in Fig. 9(a).

In summary, while load shedding is an inevitable remedial action when the power system is under stress, it has a negative impact on the electricity market, when it comes to the CBs. This matches our analysis in Sections III-D and IV-B.

C. Convergence Bids: Response of the ISO

The real-world results in Section V-B confirm "the issue" that we explained through mathematical analysis in Section III-D. This is not desirable and it raises the question on *how should the ISO respond to such circumstances?*

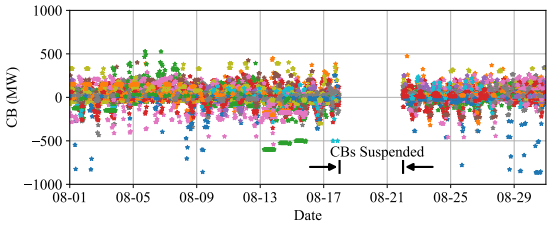

Fig. 10. Hourly cleared CBs in August 2020 in the California ISO market. CBs were *suspended* during August 18 to August 21.

Importantly, during the period from August 18 till August 21, i.e., shortly after the severe power outages, CBs were *entirely suspended* in the California ISO market. CBs were permitted again after August 21, i.e., after the level of outages almost returned to its normal level, as we saw in Fig. 7.

Fig. 10 shows all the cleared CBs in the California ISO market during the month of August. A total of 81 CB market participants had at least one cleared bid in August 2020; and each color in this figure is associated with one of the market participants. As we can see, there is no cleared CB during August 18 to August 21, as convergence bidding was fully suspended for the entire day on these four days.

It should be emphasized that the California ISO has the authority to suspend CBs when necessary per Tariff Section 7.9. This can be performed to bids already submitted or to bids that will be submitted in the future at any node [30].

While the reasoning for the California ISO's decision about suspending the CBs is *not* disclosed in details, e.g., see [28], this real-world decision *does* very well match our conclusions that we obtained mathematically in Sections III and IV.

VI. Conclusions and Future Work

This paper addressed the open problem of understanding the operation and impact of CBs during blackouts. A new functional approach as well a new metric were introduced to determine whether a given CB exacerbates or heales the blackout. A series of mathematical theorems were developed and numerical analysis were conducted under different network conditions. It was shown that supply CBs typically hurt the system during blackouts while demand CBs typically help the system. The impact of load shedding on the profit of CBs was also investigated. It was shown that, load shedding usually creates advantage for supply CBs and disadvantage for demand CBs in terms of their profit. The combination of these various results raised the issue on whether the operation of CBs is fair and justified during the blackouts. Therefore, to gain more insights, we also analyzed the real-world market data from the California ISO during the blackouts in August 2020. It was shown that, the decision by the California ISO to suspend CBs during this event is justified and it matches the mathematical and numerical results that were obtained in this paper.

This paper can be extended in various directions. First, there exist mechanisms that are used by some ISOs that can have impact on the operation of CBs during blackouts. One example for such mechanism is the use of "scarcity pricing". The impact of scarcity pricing can be investigated in the

future. Second, while our system model considers the most fundamental components of the problem formulation in two-settlement electricity markets, other components can be added to problem formulation to expand this analysis in the future, such as by using nonlinear power flow equations, incorporating power loss, and adding the voltage constraints. Third, other alternative formulations for the analysis of load shedding can also be considered. For example, there are ideas to incorporate cost efficiency in deciding the amount of load shedding during blackouts. While the credibility of such considerations should be examined, they can affect the results in different directions.

REFERENCES

[1] W. Hogan, "Virtual bidding and electricity market design," *The Electricity Journal*, vol. 29, no. 5, pp. 33–47, 2016.

[2] J. Parsons, C. Colbert, J. Larrieu, T. Martin, and E. Mastrangelo, "Financial arbitrage and efficient dispatch in wholesale electricity markets," *MIT Center for Energy and Environmental Policy Research*, 2015.

[3] Defining convergence (virtual) bidding in California ISO, [Online]: https://www.caiso.com/Documents/ConvergenceBiddingSession1-DefiningConvergenceBidding.pdf.

[4] J. Kazempour and B. F. Hobbs, "Value of flexible resources, virtual bidding, and self-Scheduling in two-settlement electricity markets with wind generation - part I: principles and competitive model," *IEEE Trans. on Power Systems*, vol. 33, no. 1, pp. 749–759, 2017.

[5] C. K. Woo, J. Zarnikau, E. Cutter, S. Ho, and H. Leung, "Virtual bidding, wind generation and California's day-ahead electricity forward premium," *The Electricity Journal*, vol. 28, no. 1, pp. 29–48, 2015.

[6] M. Kohansal, E. Samani, and H. Mohsenian-Rad, "Understanding the structural characteristics of convergence bidding in nodal electricity market," *IEEE Trans. on Ind. Informatics*, vol. 17, pp. 124–134, 2021.

[7] Y. Wang, C. Chen, J. Wang, and R. Baldick, "Research on resilience of power systems under natural disasters—a review," *IEEE Trans. on Power Systems*, vol. 31, no. 2, pp. 1604–1613, 2015.

[8] R. Li, A. Svoboda, and S. Oren, "Efficiency impact of convergence bidding in the California electricity market," *Journal of Regulatory Economics*, vol. 48, no. 3, pp. 245–284, 2015.

[9] L. Hadsell, "The impact of virtual bidding on price volatility in New York's wholesale electricity market," *Economics Letters*, vol. 95, no. 1, pp. 66–72, 2007.

[10] P. You, D. F. Gayme, and E. Mallada, "The role of strategic load participants in two-stage settlement electricity markets," in *Proc. of the IEEE Conference on Decision and Control (CDC)*, Nice, France, 2019.

[11] A. Long and A. Giacomoni, "Exploring the impacts of virtual transactions in the PJM wholesale energy market," in *Proc. of the IEEE PES General Meeting*, Montreal, Canada, 2020.

[12] S. Ledgerwood and J. Pfeifenberger, "Using virtual bids to manipulate the value of financial transmission rights," *The Electricity Journal*, vol. 26, no. 9, pp. 9–25, 2013.

[13] A. Tajer, "False data injection attacks in electricity markets by limited adversaries: stochastic robustness," *IEEE Trans. on Smart Grid*, vol. 10, no. 1, pp. 128–138, 2017.

[14] S. Baltaoglu, L. Tong, and Q. Zhao, "Algorithmic bidding for virtual trading in electricity markets," *IEEE Trans. on Power Systems*, vol. 34, no. 1, pp. 535–543, 2018.

[15] D. Xiao, J. C. do Prado, and W. Qiao, "Optimal joint demand and virtual bidding for a strategic retailer in the short-term electricity market," *Electric Power Systems Research*, vol. 190, 2021.

[16] E. Samani and H. Mohsenian-Rad, "A data-driven study to discover, characterize, and classify convergence bidding strategies in California ISO energy market," in *Proc. of IEEE PES Innovative Smart Grid Technologies Conference (ISGT)*, 2021, address=Washington, DC,.

[17] E. Samani, M. Kohansal, and H. Mohsenian-Rad, "A data-driven convergence bidding strategy based on reverse engineering of market participants performance: A case of California ISO," *IEEE Trans. on Power Systems*, 2022.

[18] Scarcity Pricing Background Discussion, [Online]: http://www.caiso.com/Documents/ScarcityPricingBackgroundDiscussionHarvey-Presentation-Dec11_2020.pdf.

[19] Price Formation Enhancements Discussion, [Online]: http://www.caiso.com/Documents/new-initiative-price-formation-enhancements-call-on-071222.html.

[20] Price Formation Enhancements Issue Paper, [Online]: http://www.caiso.com/InitiativeDocuments/Issue-Paper-Price-Formation-Enhancements.pdf.

[21] Opinion on Market Enhancements for Summer 2021 Readiness, [Online]: http://www.caiso.com/Documents/MSCOpinionon MarketEnhancementsfor2021SummerReadiness-Mar8_2021.pdf.

[22] http://www.caiso.com/CBT/MasterFileProcess/MasterFileProcess.html.

[23] E. Samani and F. Aminifar, "Tri-level robust investment planning of DERs in distribution networks with AC constraints," *IEEE Trans. on Power Systems*, vol. 34, no. 5, pp. 3749–3757, 2019.

[24] S. Boyd and L. Vandenberghe, *Convex optimization*. Cambridge university press, 2004.

[25] Y. Fu and Z. Li, "Different models and properties on lmp calculations," in *Proc. of the IEEE PES General Meeting*, Montreal, Canada, 2006.

[26] P. A. Ruiz, E. Goldis, A. M. Rudkevich, M. C. Caramanis, C. R. Philbrick, and J. M. Foster, "Security-constrained transmission topology control milp formulation using sensitivity factors," *IEEE Trans. on Power Systems*, vol. 32, no. 2, pp. 1597–1605, 2016.

[27] Power Systems Test Case Archive, [Online]: https://labs.ece.uw.edu/pstca/pf14/pg_tca14bus.htm.

[28] Final Root Cause Analysis Mid-August 2020 Extreme Heat Wave, [Online]: http://www.caiso.com/Documents/Final-Root-Cause-Analysis-Mid-August-2020-Extreme-Heat-Wave.pdf.

[29] PowerOutage.US, [Online]: https://poweroutage.us.

[30] California Independent System Operator Corporation Fifth Replacement FERC Electric Tariff, [Online]: http://www.caiso.com/Documents/Conformed-Tariff-as-of-Dec15-2021.pdf.

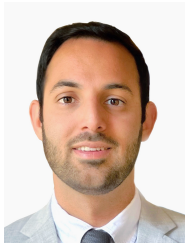

Ehsan Samani (S'16) received the B.Sc. and M.Sc. degrees in electrical engineering from the University of Tehran and the Ph.D. degree in electrical engineering from the University of California, Riverside. His research interests include analyzing different aspects of power markets, energy storage systems, renewable energies, and virtual bidding in wholesale electricity markets using data analysis, mathematical modeling, optimization methods, and machine learning techniques. His Ph.D. dissertation is focused on analyzing convergence bidding in wholesale electricity markets. He has recently joined the ICF International Inc as a Senior Consultant focusing on power markets.

Hamed Mohsenian-Rad (M'09-SM'14-F'20) received the Ph.D. degree in electrical and computer engineering from the University of British Columbia, Vancouver, BC, Canada, in 2008. He is currently a Professor of electrical engineering and a Bourns Family Faculty Fellow at the University of California, Riverside, CA, USA. His research is on monitoring, data analysis, and optimization of power systems and smart grids. He is the author of the textbook *Smart Grid Sensors: Principles and Applications* by Cambridge University Press - 2022. He was the recipient of the National Science Foundation (NSF) CAREER Award, the Best Paper Award from the IEEE Power & Energy Society General Meeting, the Best Paper Award from the IEEE Conference on Smart Grid Communications, and a Technical Achievement Award from the IEEE Communications Society. He has been the PI on ten million dollars research grants in the area of smart grid. He has served as Editor for the IEEE TRANSACTIONS ON POWER SYSTEMS, IEEE TRANSACTIONS ON SMART GRID and the IEEE POWER ENGINEERING LETTERS.